



Supplement of

A satellite observation-based analysis of cirrus ice crystal number concentrations and underlying cirrus formation mechanisms over the Tibetan Plateau

Kai Wang et al.

Correspondence to: Qianshan He (oxeye75@163.com)

The copyright of individual parts of the supplement might differ from the article licence.

This file includes Supplementary Figs. S1–S7, which can be presented as follows:

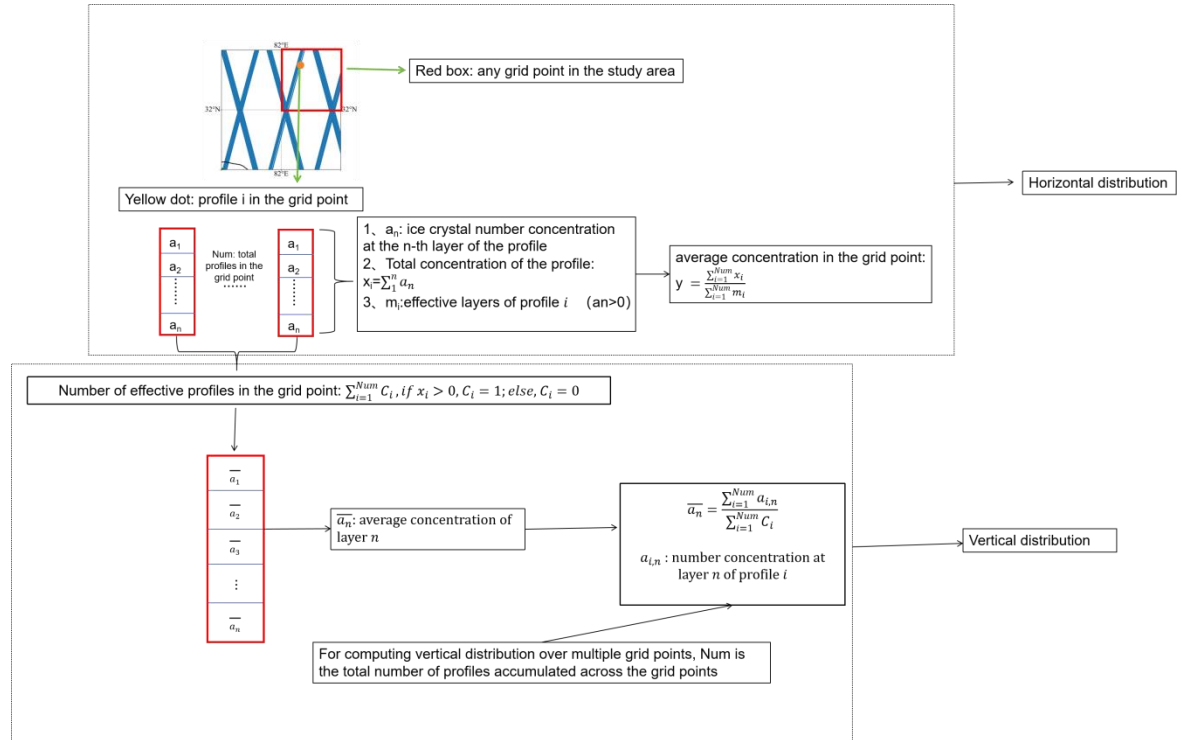


Fig. S1. Procedure for deriving N_i statistics, including calculations in both the horizontal and vertical directions.

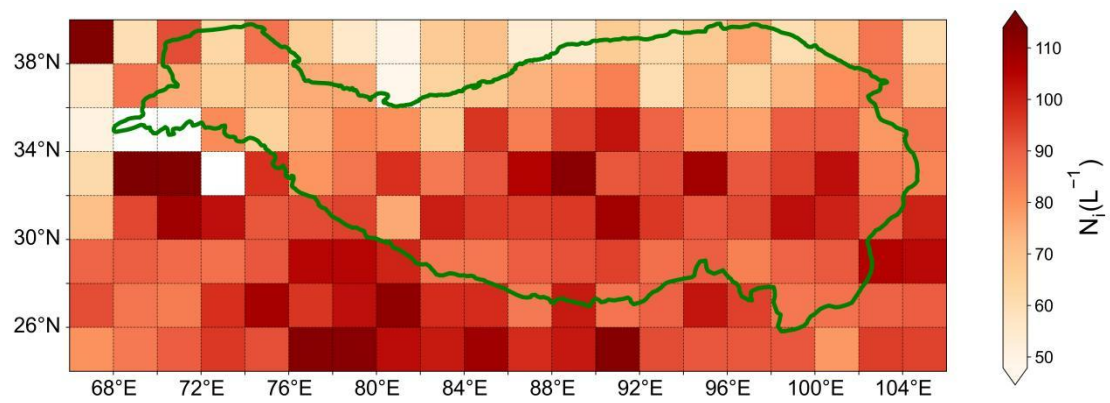


Fig. S3. Horizontal distribution of the averaged $N_i (>25 \text{ um})$ during the summer from 2006 to 2016 (except 2011) over the TP. The green line is the border of the TP.

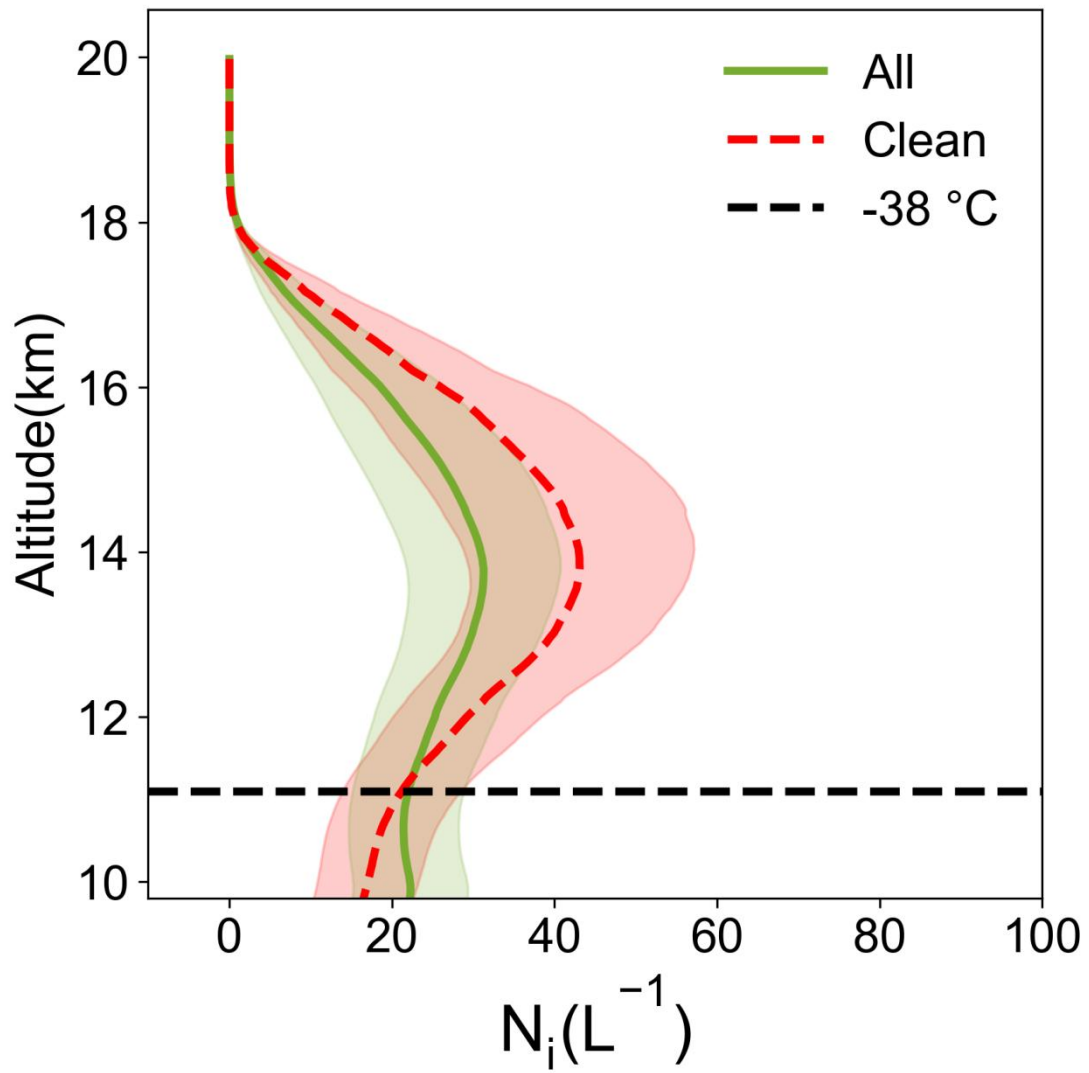


Fig. S4. Vertical profiles of $N_i (>25 \text{ um})$ for all satellite-retrieved cases ('all') and for clean aerosol conditions ('clean'), with light shading indicating the standard error range.

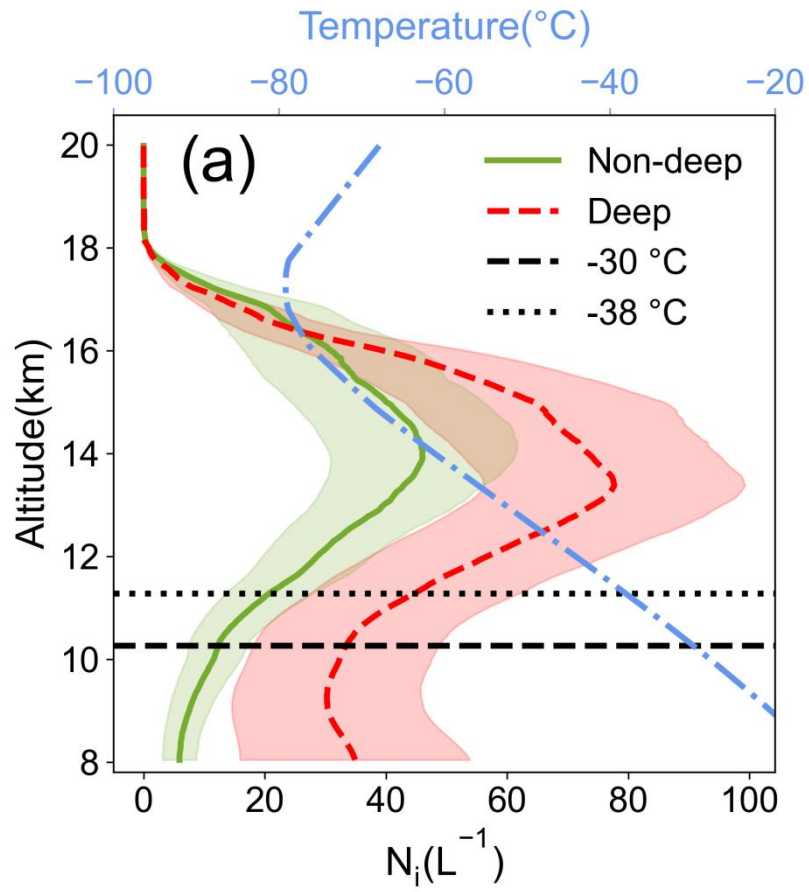


Fig. S5. Vertical profile of the $N_i (>25 \text{ um})$ affected by DCO.

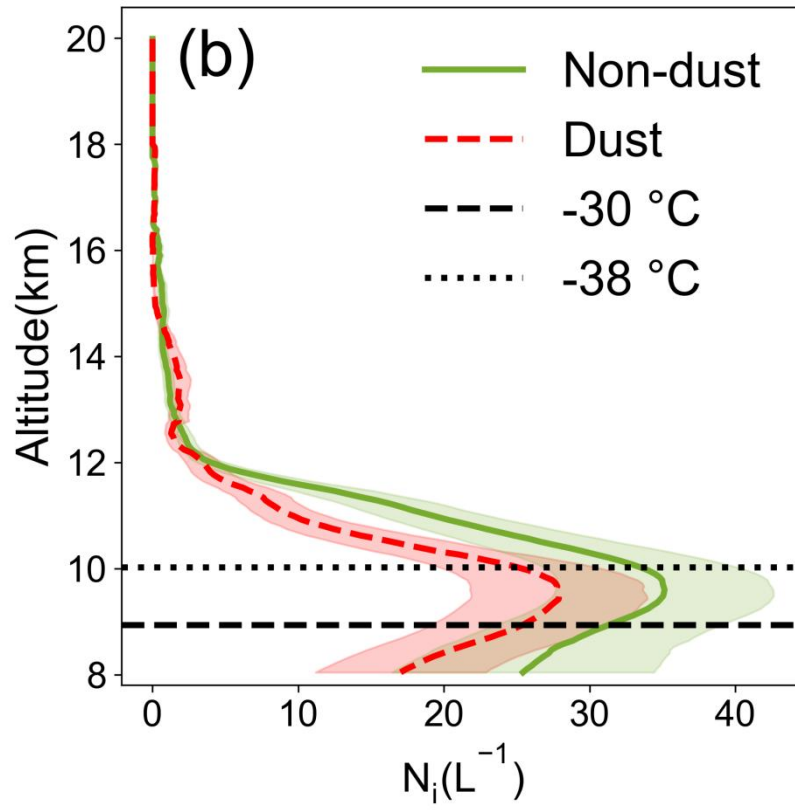


Fig. S6. The vertical profile of the N_i ($>25 \mu\text{m}$) affected by dust and non-dust events. Here, ‘non-dust’ refers to all cases in which CALIPSO does not detect dust aerosols, including clean aerosol conditions.

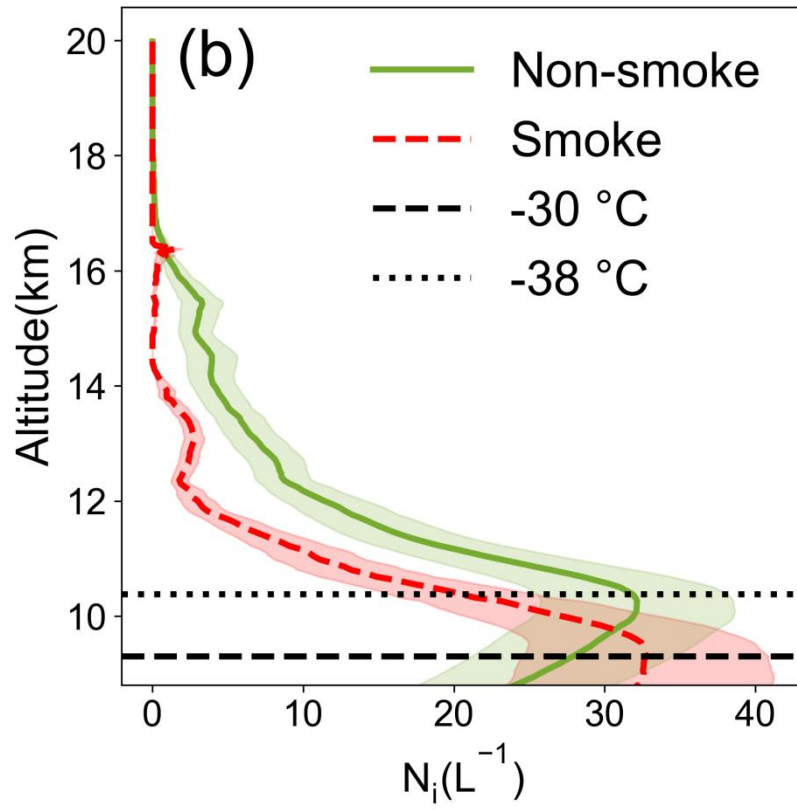


Fig. S7. The vertical profile of the $N_i (>25 \text{ um})$ affected by smoke and non-smoke events. Here, 'non-smoke' refers to all cases in which CALIPSO does not detect smoke aerosols, including clean aerosol conditions.